



**Optical chirality sensing using macrocycles, synthetic and supramolecular oligomers/polymers, and nanoparticles based sensors**

Journal:	<i>Chemical Society Reviews</i>
Manuscript ID:	CS-REV-12-2014-000531.R1
Article Type:	Tutorial Review
Date Submitted by the Author:	31-Dec-2014
Complete List of Authors:	Chen, Zhan; Xiamen University, Department of Chemistry Wang, Qian; Xiamen University, Department of Chemistry Wu, Xin; Xiamen University, Department of Chemistry Li, Zhao; Xiamen University, Department of Chemistry Jiang, Yun-Bao; Xiamen University, Department of Chemistry

## ARTICLE

Cite this: DOI: 10.1039/x0xx00000x

**Optical chirality sensing using macrocycles, synthetic and supramolecular oligomers/polymers, and nanoparticles based sensors**Received 00th January 2012,  
Accepted 00th January 2012

DOI: 10.1039/x0xx00000x

[www.rsc.org/](http://www.rsc.org/)Zhan Chen,<sup>a</sup> Qian Wang,<sup>a</sup> Xin Wu,<sup>a</sup> Zhao Li<sup>a</sup> and Yun-Bao Jiang<sup>a,\*</sup>

Optical sensors that respond to enantiomeric excess of chiral analytes are highly demanded in chirality related research fields and demonstrate their potentials on many subjects, for example, screening of asymmetric reaction products. Most sensors developed so far are small molecules. This *Tutorial Review* covers recent advances in chirality sensing systems that are different from the traditional small molecule-based sensors, by using macrocycles, synthetic oligomers/polymers, supramolecular polymers and nanoparticles as the sensors, in which supramolecular interactions are operating.

**Key learning points:**

Two major approaches to chirality sensing, *i.e.*, using chiral sensors that form diastereomeric complexes with chiral analytes and using achiral or dynamically racemic sensors that exhibit induced chirality upon analyte binding.

Versatile sensing ensembles based on macrocyclic hosts that have a cavity for chiral auxiliary, chiral analytes or reporting dye.

Synthetic or supramolecular polymers that show chiral analyte induced helical chirality.

Chirality sensing based on chiral analyte-dependent nanoparticle assembly.

**Introduction**

Within the area of chemical sensing, there has been considerable interest in designing synthetic optical sensors that effectively discriminate between enantiomers of a certain class of chiral compounds.<sup>1-3</sup> Those sensors, here referred to as chirality sensors, are designed to interact with chiral analytes *via* covalent or noncovalent interactions, giving spectroscopic responses that depend on the enantiomeric excess (*ee*) of the tested chiral analytes. These sensors have shown their potentials in many fields where chirality is an important parameter, for instance, they have dramatically facilitated the development of asymmetric syntheses by offering effective means of determining *ee* of the reaction products. In the case of optical sensors, given that the sensor-analyte interactions take place fast enough, which is usually not a problem for supramolecular sensors, the rapidness and relatively low cost of spectroscopic assays will confer great advantages over prevailing methods such as chromatographic techniques,

(*iChEM*), Xiamen University, Xiamen 361005, China. \* E-mail: [ybjjiang@xmu.edu.cn](mailto:ybjjiang@xmu.edu.cn).

especially when hundreds of reaction products need to be quickly analyzed to optimize the reaction conditions.

Chirality sensing is to distinguish right-handed and left-handed chirality and/or to determine the optical purity of chiral samples. There are two major approaches to discriminate between enantiomers by (i) using chiral sensors<sup>1</sup> that forms diastereomeric sensor-analyte complexes giving different UV-Vis absorption, fluorescence or NMR responses, and (ii) using achiral sensors<sup>3</sup> that show induced chirality upon sensor-analyte interactions that give responses detectable by a chiral discriminating spectroscopy such as CD or circularly polarized luminescence (CPL). A third, less common approach also exists, which does not involve the use of any chiral auxiliary or chiral discriminating spectroscopy, but is based on a specific interaction of the sensor with (*R*)- and (*S*)-analytes by forming molecular complexes or assemblies that generate an *ee*-dependent response in a spectroscopic instrument that possesses no intrinsic chiral discriminating capacity.<sup>4-6</sup>

Most of the chirality sensors so far designed, by any of the three approaches described above, are based on small molecules, which have already been covered by several excellent comprehensive reviews,<sup>1-3</sup> therefore they are not

<sup>a</sup> Department of Chemistry, College of Chemistry and Chemical Engineering, MOE Key Laboratory of Spectrochemical Analysis and Instrumentation, and Collaborative Innovation Center of Chemistry for Energy Materials

discussed here. In spite of the great success achieved with those small-molecule based sensors, often, an elaborately designed sensor structure is required. In the case of chiral sensors, (i) the differences in association constants of the diastereomeric sensor-analyte complexes should be sufficiently large, if the resulting diastereomeric complexes possess identical UV-Vis absorption or fluorescence spectra; or (ii) alternatively, the spectroscopic properties of the diastereomeric complexes should be different to allow discrimination by UV-Vis absorption, fluorescence or NMR methods. In the case of achiral sensors, they may be flexible in their conformation or exist as a racemic mixture of rapidly inter-converting enantiomeric conformers. Upon chiral analyte binding, the conformation of the sensor molecule should be effectively restricted that results in chirality induction, or the energy difference between the diastereomeric conformers should be sufficiently large to bias the formation of either conformer, leading to nonracemic composition of the conformers that might be probed by spectral responses.

Recently, new concepts have been introduced to the area of optical chirality sensing. Instead of using small molecules, supermolecules are designed as sensors for chirality sensing. Macrocyclic hosts that have a cavity, either achiral or chiral, may provide sensing properties that cannot be achieved by small molecules. For example, the large cavity of cucurbiturils and cyclodextrins may allow inclusion of multiple guest molecules, while the interactions among the entrapped guest molecules can be exploited to design simple chirality sensing ensembles, without the need of covalently conjugating analyte binding site to the sensor molecule.

Certain synthetic oligomers and polymers are known to exist in helical structures. For example, synthetic oligomers in suitable solvents can undergo folding in a helical fashion, driven by intramolecular hydrogen bonding and/or solvophobic interactions. Macromolecular helicity can also result from synthetic polymers possessing bulky side chains that create higher rotation energy barriers. These helical oligomers or polymers are dynamically racemic in the absence of any external influence, while simple sensor design can allow single-helicity induction by analyte binding. Alternatively, those helical oligomers or polymers bearing chiral substituents selectively form a cavity with single helicity, which thereby binds chiral guest molecules in an enantioselective manner.

A seemingly promising, yet not fully exploited platform for chirality sensing is that employs supramolecular polymers formed by self-assembly of small building blocks, such as aggregates of  $\pi$ -conjugated dye molecules, Langmuir-Blodgett films, supramolecular gels, and coordination polymers. Similar to synthetic oligomers or polymers, supramolecular polymers can easily possess helical structures, exhibiting “supramolecular chirality” as distinct from the “molecular chirality”. Yet the supramolecular polymers are formed via noncovalent interactions among the building blocks, the latter is hence much easier to design and synthesize than synthetic oligomers/polymers. This may facilitate sensor design and optimization, for example to achieve spectral responses in long

wavelength window to minimize interference from impurities or chiral catalysts from asymmetric syntheses. Beside the structural diversity of the building blocks, the higher local concentration of the binding sites and the relative orientation between them that can be tuned good for analyte binding are the additional advantageous characters that the supramolecular polymer based sensors can offer. In both synthetic and supramolecular polymer based sensors the possible cooperative interactions occurring between the sensor and analyte molecules may afford chirality amplification that could be employed to design chirality sensing systems with higher sensitivity and accuracy as well.

Finally, the unique self-assembling capabilities and spectral properties of nanoparticles can be utilized in the design of highly sensitive chirality sensors, as they have proved potent in bio-sensing and imaging. The nanoparticles themselves can also be signal reporter and the structural framework to load ligand molecules on the surfaces in the manners that could in principle be made good for chirality sensing.

Compared to the small-molecule based sensors, chirality sensing in these four supramolecular systems exhibits unique characteristics. In general, sensors established on the basis of various cooperative interactions provide more chances for mirror-symmetry-break. In fact, “sergeant and soldiers” and “majority rule” effects often are observed in these systems because of the efficient chiral amplification. Small *ee* could therefore be determined more sensitively than that in the small-molecule sensory systems. In addition, the establishment of hierarchical chiral systems may further enhance the sensitivity for detecting and quantifying chirality. On the other hand, drawbacks exist either. The S-shaped chiroptical response to *ee* due to chiral amplification is powerless for sensing *ee* above 95% or below 5%. In the cases of polymeric systems and nanomaterials, the sample preparation might be lengthy in order to obtain a stable and reproducible optical response. Also those oligomer or polymer sensors might be sensitive to environmental conditions such as temperature, ionic strength, and the presence of impurities, which could limit the practical applications.

In this *Tutorial Review*, we will describe those four classes of chirality sensors and discuss the mechanisms on which they operate to afford interesting chirality sensing performances that are different from the traditional small-molecule based chirality sensors.

## Macrocycles

Macrocyclic sensors here refer to as barrel-shaped compounds with a cavity. It is because of this cavity, its size and hydrophobicity or hydrophilicity, that these macrocyclic sensors are able to accommodate multiple guest molecules within the cavity, which is intriguing for chirality sensing in several ways. These guest molecules may include chiral analyte, chiral molecule responsible for enantioselective binding with the chiral analyte, and/or chromophore responsible for generating spectroscopic outputs. By assembling those

species within a macrocyclic host, synthetic efforts to covalently conjugate them are not needed, while more flexible and versatile sensing schemes can be designed.

The macrocyclic sensors can be themselves chiral or achiral. Achiral cucurbituril sensors represent a kind of active current interest. Inoue *et al.*<sup>7</sup> examined the enantioselective guest recognition of cucurbituril hosts. The enantioselectivity relies on the inclusion of a chiral auxiliary to form ternary diastereomeric complexes of the analyte. Cucurbit[6]uril (CB[6]) and the chiral auxiliary 2-methylpiperazine (MP) forms a 1:2 inclusion complex in aqueous solution (Fig. 1). Guest molecule 2-methylbutylamine (MB) replaces one of the MPs from the CB[6] cavity, forming a ternary  $[\text{CB}[6]\cdot[\text{MP}]\cdot[\text{MB}]]^{3+}$  complex with enantioselectivities. This ensemble exhibits a remarkable 19-fold selectivity for the formation of  $[\text{CB}[6]\cdot(R)\text{-MP}\cdot(S)\text{-MB}]$  complex over its diastereomer  $[\text{CB}[6]\cdot(S)\text{-MP}\cdot(S)\text{-MB}]$ , evaluated from the isothermal titration calorimetry (ITC) measurements. The enantioselectivity was explained in terms of a larger enthalpy loss in the case of forming  $[\text{CB}[6]\cdot(S)\text{-MP}\cdot(S)\text{-MB}]$  complex due to more severe distortion of MP positioning within the CB cavity from its original optimal location. Although the system does not show any spectroscopic output and the scope of the analytes is limited, it demonstrates a promising strategy on which more practically useful sensing schemes can be based, by for example, using an indicator displacement assay. It also suggests the role of geometric factors of the included molecules within the cavity.

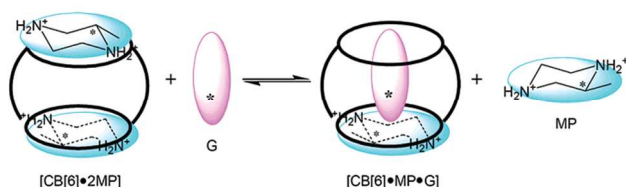


**Fig. 1** Enantioselective recognition of guest molecules (G) by cucurbit[6]uril [CB(6)] and a chiral auxiliary 2-methylpiperazine (MP). (Reprinted with permission from *J. Am. Chem. Soc.*, 2006, **128**, 14871-14880. Copyright 2006 ACS).

Nau and coworkers have recently developed two different chirality sensing assays based on the inclusion complexes of cucurbituril hosts and dye molecules, that act as spectroscopic reporters. One of them employed the stereospecific enzymatic reactions (Fig. 2).<sup>8</sup> Enzymes able to convert specifically the L-enantiomers of amino acids to amines were chosen, following the fact that the amines show significantly higher affinities towards CB[7] host than the amino acid substrates. Therefore, at suitable substrate concentrations, the amine produced by the enzymatic reactions, but not the amino acid substrate, displaces the fluorescent dye Dapoxyl previously included within the CB[7] cavity, leading to quenching of Dapoxyl fluorescence. When a mixture of enantiomers was subject to the analysis, the extent of fluorescence quenching depends on *ee* of the analytes. Because of the stereospecificity of enzymatic reactions and the sensitivity of the fluorescent assay, accurate measurement of *ee* higher than 99% is made possible by using a high analyte

concentration. Such assays for the high end of *ee* are not achieved with traditional small-molecule based sensors.

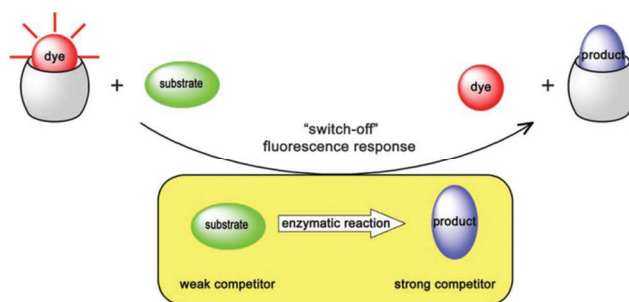


**Fig. 2** Chirality sensing by using an indicator displacement system involving a cucurbituril-dye complex coupled to an enzymatic reaction. (Reprinted with permission from *Chem. Eur. J.*, 2008, **14**, 6069-6077. Copyright 2008Wiley-VCH).

Another one from the Nau group is a CD-based chirality sensing assay that relies on the formation of ternary complex among achiral CB[8], achiral dye and the chiral analyte (Fig. 3).<sup>9</sup> The CB[8]-dye complex remains achiral and thus is CD silent, while the co-inclusion of a chiral aromatic analyte inside the CB[8] cavity effectively induces strong CD signal in the dye absorption region. The CD signal depends linearly on the *ee* of chiral analyte. This assay applied for a broad scope of analytes since it relies on non-covalent interaction between the CB host and the aromatic moieties of the guest molecules. This is a significant breakthrough compared to that based on small-molecule based sensors that require certain reactive functional groups to be present in the analyte. The assay is operable for micromolar concentrations of analytes and can be used for real time monitoring of chemical reactions, for example, the racemization of (*S*)-1-phenylethanol catalyzed by an amberlyst.

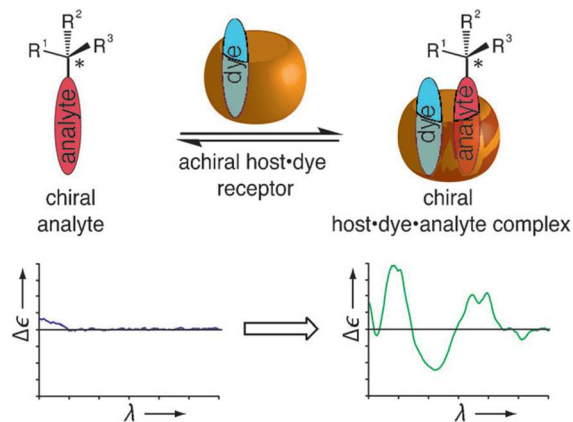


**Fig. 3** Chirality sensing based on circular dichroism (ICD) signal induced by co-inclusion of a dye and a chiral analyte inside achiral cucurbituril cavity. (Reprinted with permission from *Angew. Chem. Int. Ed.*, 2014, **53**, 5694-5699. Copyright 2014 Wiley-VCH).

It is quite surprising that other macrocycles<sup>10,11</sup> have not been paid much attention, in particular the cyclodextrins that have a chiral cavity, despite the facts that multi-point interactions between guest molecules included within the chiral cavity of cyclodextrin have been shown to induce supramolecular

chirality from the achiral guest.<sup>12,13</sup> This actually results from tight package within the chiral space of cyclodextrin cavity by more than one guest molecules. In this case at least one guest molecule acts as a spacer that helps to fill the cavity, a mechanism that has been popular since the 1990's for creating cyclodextrin-based room-temperature phosphorescence (RTP) systems, using for example a third component to enhance the RTP of bromonaphthalenes in aqueous cyclodextrin solutions.<sup>14</sup> This actually opens up a new entry to chirality sensing by using cyclodextrin if the third component is the chiral analyte, as shown in this example.

Regarding the macrocycle-based chirality sensing systems here we emphasize those where the cavity includes more than one guest molecules (including the chiral analyte) that the sensor affords additional advantages benefiting from the cavity size and its hydrophobicity or hydrophilicity, while the ensemble is formed by the coupled supramolecular interactions among the guest molecules and the cavity.

### Synthetic oligomers/polymers

Some of the polymers exist in helical conformation with the same amount left- and right-handed conformers, which equilibrium can be biased by the presence of a chiral analyte that interacts with the polymer. Quite often the so-called "majority-rules" effect was observed,<sup>15</sup> in which a small *ee* produces a non-proportionally large CD signal, and thus the CD-*ee* curve shows a steeper slope around 0% *ee*. This phenomenon has been proposed by Yashima *et al.*<sup>16</sup> to be applicable to the determination of a small enantiomeric imbalance. The working system is a stereoregular *cis*-transoidal poly(phenylacetylene) **1** consisting of a polyacetylene backbone as the chromophore and bulky crown ether as the pendant binding unit for amino acid (Fig. 4). Upon binding to L- and D-alanine (Ala), **1** exhibits strong chiral amplification which was apparent even with 0.01 equiv of L-Ala. An extremely strong "majority-rules" effect was observed and 5% *ee* of Ala was able to generate full ICD signal. Detection of extremely small enantiomeric excess of 0.005% of Ala is possible. This system has been successfully applied to 19 L-amino acids as well as 5 chiral amino alcohols.

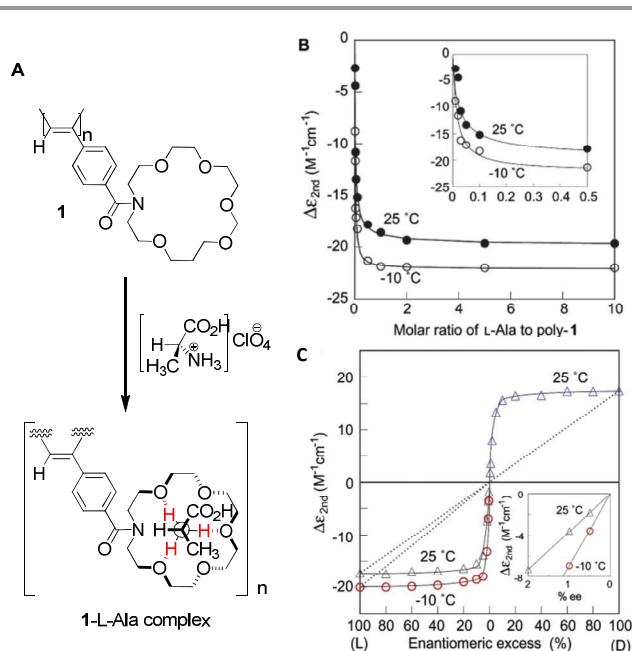
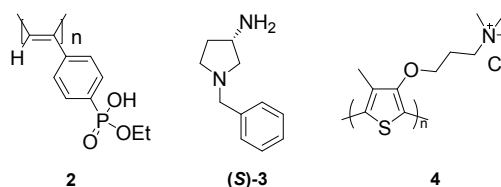


**Fig. 4** (A) Poly-1 and its interaction with L-Alanine. (B) Titration curves of poly-1 vs molar ratio of L-Ala•HClO<sub>4</sub> in acetonitrile. (C) Changes of ICD intensity of poly-1 vs % *ee* of L-Ala•HClO<sub>4</sub>. (Reprinted with permission from *J. Am. Chem. Soc.*, 2002, **125**, 1278-1283. Copyright 2003 ACS).

Using the same concept of design, a stereoregular *cis*-transoidal poly(phenylacetylene) bearing a phosphoric acid monoethyl ester pendant was shown to form preferred helicity upon complexation with a series of optically active pyrrolines and piperazines in DMSO and in water.<sup>17</sup> Strong chiral amplification was observed for **2** upon binding to (*S*)-**3**. The "majority-rules" effect is not as strong as that observed with **1**, 40%-60% *ee* of (*S*)-**3** is needed to generate full ICD signal. Lyotropic nematic and cholesteric liquid crystalline phases were observed for **2** in the presence of chiral amines. It shall be pointed out that the nematic and cholesteric liquid crystallines showed almost the same X-ray diffraction patterns, which indicates that the dynamically racemic and one-handed helices have the same helical structure, a hint that may help understand the operation mechanism. An issue that remains uncertain is the prediction of the occurrence or not of chiral amplification in the polymer based chirality sensors. This also exists with oligomer and supramolecular polymer based sensors, which will be discussed later in this *Review*, since the mechanism of chiral amplification remains unclarified.



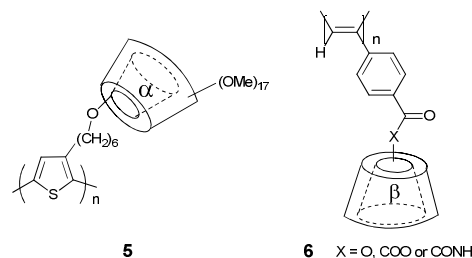
Detection of high *ee* close to 100% is however more important in asymmetric syntheses. Anslyn *et al.*<sup>18</sup> recently developed a new concept of measuring *ee* higher than 95% with lower errors, using the "majority-rules" active polymer **1** previously reported from the group of Yashima.<sup>16</sup> By adding an

equivalent amount of the opposite enantiomer, the high *ee* value of the sample was converted into low *ee*, thus cleverly employing the sensitive high slope of the low *ee* region (refer to Fig. 4c). The calibration curve exhibited a slope of 6.2 mdeg/(% *ee*), which is higher than the slope of linear response (1.3 mdeg/(% *ee*)) obtained in the same range of Yashima's system. For sample, with *ee* values from 95% to 100%, remarkably low errors were found, lower than commonly reported chiral HPLC error values of 0.5 to 1%. This system could well detect *ee*'s over 95%, at lower *ee* values larger errors however were observed. Meanwhile, the instability of the polymers necessitates the development of a more robust system for further practical applications.

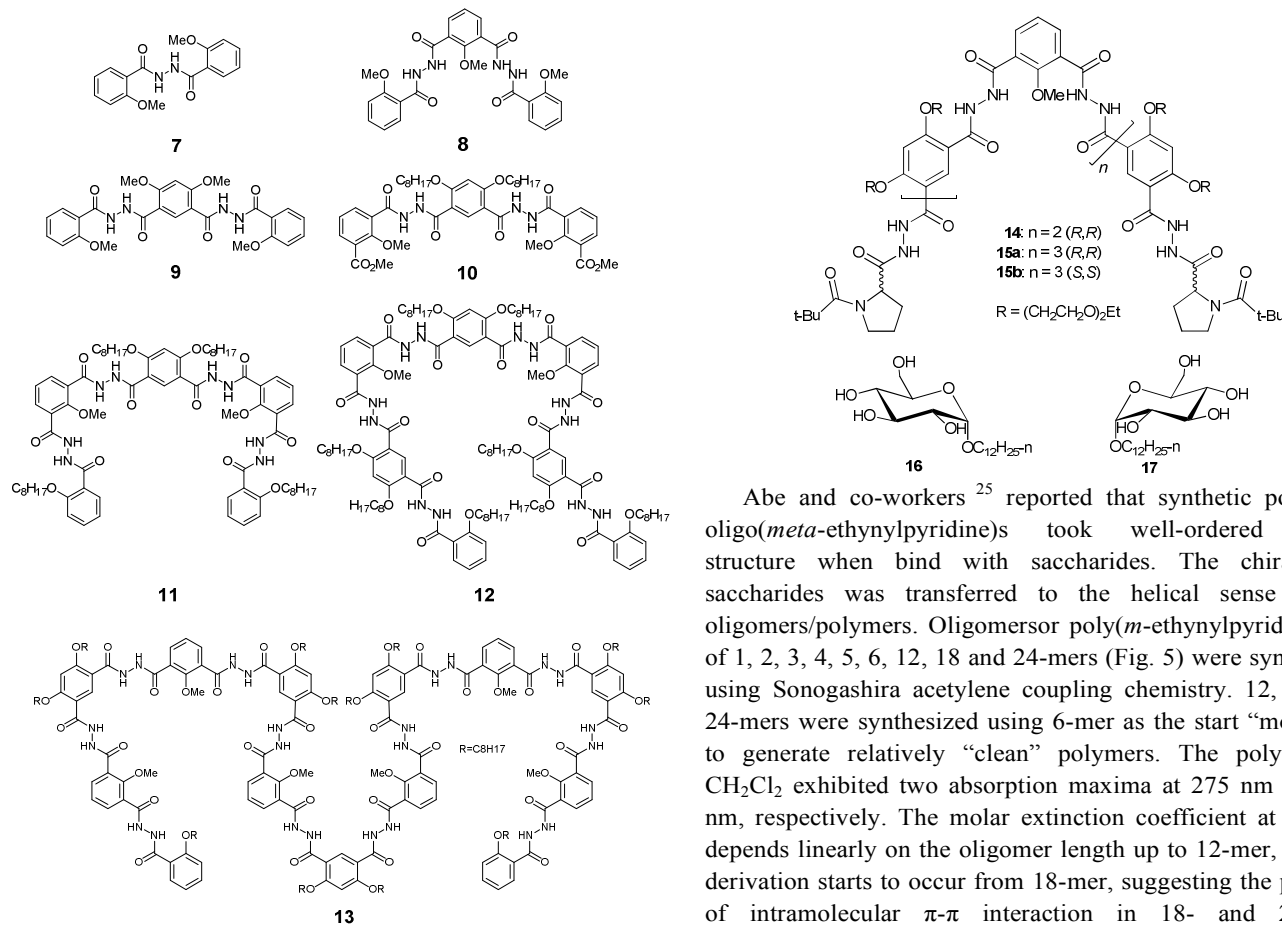
Shinkai *et al.*<sup>19</sup> observed an unexpected chirality induction from cationic polythiophene **4** by monosaccharides. Achiral polymer **4** in a good solvent (methanol) showed peculiar CD signal when diluted with a poor solvent (chloroform) in the presence of galactose (pre-dissolved in DMSO). A colour change was observed, together with the appearance of new absorptions at 510 nm, 542 nm and 588 nm, respectively, indicating possible  $\pi$ - $\pi^*$  transitions in the formed aggregates of polymer **4**. Enantiomers of galactose, glucose and fructose generated symmetric ICD signals. The observed CD signal correlated linearly with the enantiometric ratio of galactose, which means no chiral amplification occurs in this case in which the chiral analyte seems to induce helical stacking of the polymers. More interestingly, the number of hydroxyl groups in the tested saccharides appears crucial to the ICD signals from the aggregates of **4**, since four-OH saccharides such as fucose and 2-deoxygalactose barely induces any CD signal. Thus, a multi-point hydrogen bonding mechanism was proposed for the chiral induction in **4** by saccharides. An approximately linear relationship was also observed between the optical rotation  $[\alpha]$  as the polarizability indicator and the ICD signal at 598 nm. It was hence proposed that saccharides with larger dipole moment possibly induced stronger chiral mode of **4**. This phenomenon suggested that the dipole moment difference of the saccharides could be the reason that causes diverse ICD signals upon association with **4**. The system was applied for pattern recognition of saccharides.

Achiral polymers bearing chiral pendants were also developed for chirality sensing. Polythiophene conjugated with permethyl- $\alpha$ -cyclodextrin via flexible hexamethylene chain, **5**<sup>20</sup> was found to exhibit a weak positive Cotton effect in the main absorption band of the polythiophene backbone, suggesting that the appending cyclodextrin via a long flexible chain was ineffective in inducing a homochiral structure in the polymer backbone. Yet amino acids and dipeptides indeed enable to induce chirality-dependent hypochromic changes in the absorption spectra. Enantiomeric DD/LL-dipeptide pairs were better differentiated than the D/L-amino acid pairs, with the highest DD/LL selectivity of *ca.* 14 observed with Phe-Phe dipeptides. Chirality responsive behavior of poly(phenylacetylene)s bearing  $\beta$ -cyclodextrin pendants *via* ester, ether, and amide linkages<sup>21</sup> was found linkage dependent. The amide linked polymers **6** exhibited a unique

enantioselective gelation in response to the chirality of chiral amines. It appears that the relatively rigid linkage is more effective in communicating the chirality message of the pendants into the polymer backbones. In the latter case the co-inclusion of more than one guest species within the chiral cavity of cyclodextrin may afford peculiar performance in chirality sensing, given the advantage of the poly(phenylacetylene) backbone that is known to afford chiral amplification (refer to Fig. 4C).



Given the difficulty in obtaining reproducible polymers, synthetic oligomers appear advantageous. Those with foldable conformations, termed foldamers are the major structures that have been employed to build sensors that either show induced helicity upon chiral guest binding or enantioselectively recognize chiral guests. Hydrogen bonding driven achiral hydrazide foldamers,<sup>22</sup> containing 1, 2, 4, 6 or 12 repeating dibenzolyhydrazide residues (oligomers **7**, **8-13**), were designed as candidates of saccharide receptors.<sup>23</sup> Chirality induction by alkyl-substituted mono- and di-saccharides was observed in chloroform. NMR, X-ray and IR spectroscopy reveal that, while short oligomer **7**, **8** or **10** exists in rigid and planer conformation, longer oligomers **11-13** exhibit helical conformation with a rigid cavity of diameter 10.6 to 11.1 Å. Half of the carbonyl groups orientate inwardly that bind saccharides efficiently via hydrogen bonding. Moderate ICD signals were observed from oligomers **11-13** upon binding to saccharides ( $\alpha$ -L-glucose,  $\alpha$ -D-glucose,  $\beta$ -D-ribose and  $\beta$ -maltose), which was shown by Job plot in 1:1 stoichiometry. This report highlights the importance of the helical conformation of the oligomers in the possible induction of chirality by a chiral analyte.



While saccharide binding induces chirality in helical foldamers **11-13** that have an achiral framework and originally exist as dynamic racemic mixtures, analogous helical foldamers that contain stereogenic centers could exist in a preferred handed helicity and therefore recognize chiral saccharides diastereoselectively. Wang *et al.*<sup>24</sup> synthesized three chiral aromatic hydrazide foldamers with two *R*- or *S*-proline residues incorporated at the backbone termini, which, due to their helical cavity structure, were shown to form 1:1 complexes with substituted glucose enantiomers **16** and **17** with good enantioselectivity. For example, the binding constant of **14/17** complex is 144 times higher than that of the **14/16** complex. CPK model suggests that **14**, **15a** and **15b** all exist in helical conformation facilitated by intramolecular hydrogen bonding, as also indicated by the downfield shifts of the amide proton resonances. While **15a** and **15b** show mirror-imaged CD signals, non-mirror-imaged ICD signals were observed when **16** or **17** was allowed to interact with **18** in chloroform since diastereomers were formed. Mirror-imaged ICD signals were observed for enantiomeric complexes **15a/17** and **15b/16**, **15a/16** and **15b/17**. These observations suggest the potentials in chiral sensing, for example for *ee* measurements.

Abe and co-workers<sup>25</sup> reported that synthetic poly- and oligo(*meta*-ethynylpyridine)s took well-ordered helical structure when bind with saccharides. The chirality of saccharides was transferred to the helical sense of the oligomers/polymers. Oligomers or poly(*m*-ethynylpyridine)s **18** of 1, 2, 3, 4, 5, 6, 12, 18 and 24-mers (Fig. 5) were synthesized using Sonogashira acetylene coupling chemistry. 12, 18, and 24-mers were synthesized using 6-mer as the start “monomer” to generate relatively “clean” polymers. The polymers in CH<sub>2</sub>Cl<sub>2</sub> exhibited two absorption maxima at 275 nm and 323 nm, respectively. The molar extinction coefficient at 275 nm depends linearly on the oligomer length up to 12-mer, whereas derivation starts to occur from 18-mer, suggesting the presence of intramolecular  $\pi$ - $\pi$  interaction in 18- and 24-mers. Fluorescence spectra exhibited broad featureless emission over 500 nm for 12, 18, and 24-mers, probing the intramolecular excimer nature of the emissive state. *n*-Octylglycosides were tested to interact with the CD-silent polymer at monomer unit concentration of  $1.0 \times 10^{-3}$  M, leading to the observation of characteristic ICD signals at 355-325 nm. Among all the tested *n*-octylglycosides,  $\beta$ -D-Glc **16** and  $\beta$ -L-Glc **17** generated the strongest ICD signal with the polymer. The strong ICD signal of the 24-mer upon interacting with  $\beta$ -L-Glc **17** allows the evaluation of binding stoichiometry of 1:1 and association constant of  $(1.2 \pm 0.4) \times 10^3$  M<sup>-1</sup>. The polymer remained CD silent upon addition of non-hydrogen-bonding analogue Me- $\beta$ -D-Glc, nicely supporting that the hydrogen bonding interaction of the saccharide-OH groups with the pyridine N-atoms in polymer occurs to drive the helical conformation. Native saccharides were found to induce CD signals as well.

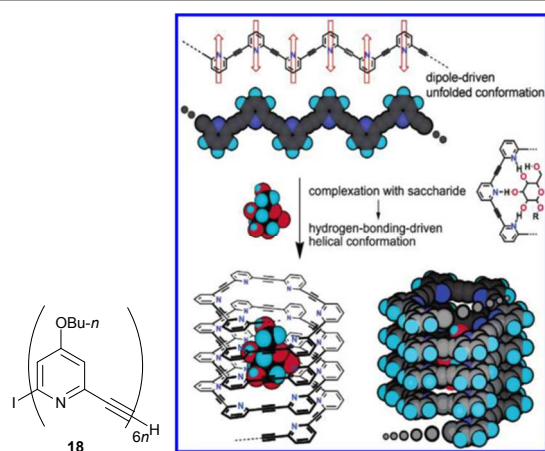


Fig. 5 Conformation change of synthetic polymer **18** driven by saccharide complexation. (Reprinted with permission from *J. Am. Chem. Soc.*, 2004, **126**, 2022–2027. Copyright 2004 ACS).

The same group also reported modification of ethynylpyridine polymer into co-oligomers which undergo dynamic transformation from self-dimers to helical complexes with saccharides (Fig. 6).<sup>26</sup> Oligomers **19–23** consist of (1H)-4-pyridone and 4-alkoxy-pyridine rings connected through acetylene bond at their 2,6-position. Vapor pressure osmometry (VPO) of oligomer **19** and its methyloxymethyl protected derivative, **19-MOM**, revealed that **19** favoured the dimer form while **19-MOM** existed in its monomer. <sup>1</sup>H NMR confirmed that the oligomers self-associated via hydrogen bonding between N atoms of the 4-alkoxy-pyridine rings and protons of (1H)-4-pyridone. Addition of octyl  $\beta$ -D-glucopyranoside to the solutions of oligomers **20–23** induced remarkable CD signals around 335 nm from the 1:1 interaction complex. Although the self-association of the oligomer itself obscured the quantitative characterization of the exact CD-active complex and remaining dimers, the dynamic transformation between CD-silent dimer and CD-active helical oligomer-saccharide complex was observed in saccharide recognition. This mechanism is of interest in that a structural change occurs upon saccharide binding, which may have resulted in an amplified signal output or better chirality sensing if allostereism would operate.

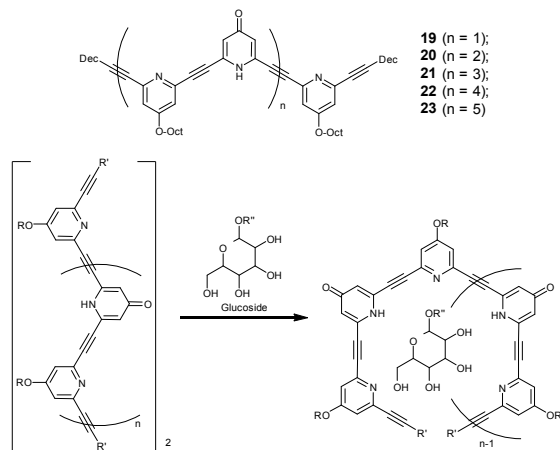
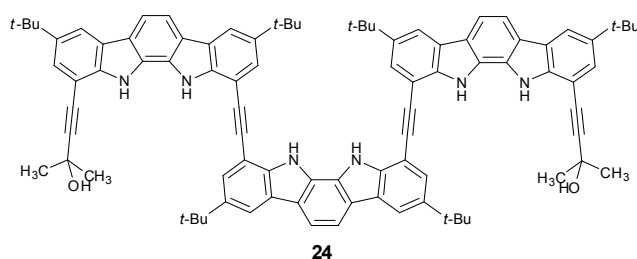


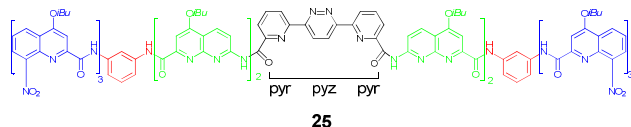
Fig. 6 Saccharide recognition by oligomers **19–23**.

Jeong *et al.*<sup>27</sup> reported an indolocarbazole foldamer **24** with larger aromatic components. It binds chiral organic ions, camphorsulfonates and cyclic monophosphate (cAMP), in the formed one-handed helical conformation. The ICD signal was found switchable through acid-base chemistry. When foldamer **24** binds with (*R*)- or (*S*)-10-camphorsulfonate, intense mirror-imaged ICD signals were observed at 362 nm, suggesting biased formation of the diastereometric helical complexes. The helical structure was further verified from the specific rotation value of (*R*)-10-camphorsulfonate which changes from  $-32^\circ$  to  $+224^\circ$  upon addition of foldamer **24**. Hydrogen bonding interaction was identified from the large downfield shifts of the pyrrolic -NH protons by 1.29, 1.73 and 2.57 ppm. The fact that the resonance signal of the aromatic CH in the central indolocarbazole was hardly shifted suggests that the two indolocarbazole rings stack to afford the helical conformation. Modelling, together with exciton chirality analysis, showed that (*R*)-10-camphorsulfonate induced *P*-helix formation in **24**. Low temperature <sup>1</sup>H NMR suggested that in the presence of (*S*)-10-camphorsulfonate, over 90% of **24** existed in one-handed helix, while the minor component was hardly detected even at  $-80^\circ\text{C}$ . TFA was able to quench the ICD signals generated from foldamer **24** and cAMP, which can be recovered by DABCO base, indicating a CD switching behaviour. This is insightful for understanding the mechanism of chiral induction in **24**. It remains not straightforward to compare the chirality sensing performance of foldamer **24** with that of the above-mentioned other foldamers, yet structurally it differs in that it contains a larger aromatic component and less repeating units, which may affords not a complete turn structure with a seemingly larger cavity.



Helically folded aromatic oligoamide **25**<sup>28</sup> represents a hetero-foldamer that consists of more than one kind of repeating units. Its hollow cavity was assumed to encapsulate tartaric acid. A long pyr-pyz-pyr linear segment was introduced to enlarge the diameter of the cavity, while the naphthyridine amide residue was incorporated to bind chiral tartaric acids. Upon addition of 1 equiv D- or L-tartaric acid, NMR signal of the free oligoamide **25** disappeared completely, indicative of a very high binding affinity. CD titration by pure D- or L-tartaric acid revealed an intense ICD signal, showing that the balance between the *M*- and *P*-forms of **25** is biased to one direction upon tartaric acid binding. Crystal structure validated that tartaric acid was completely encapsulated and surrounded by

the oligomer. Other structurally related guest molecules such as *meso*-tartaric acid that differs from D-/L-tartaric acid only in the orientation of two OH groups and D-/L-malic acid with one less OH group were also tested. The binding was found weaker, which demonstrates the high sensitivity of oligomer **25** towards a subtle difference in the chirality information of the analytes. The multiple components in the oligomer seem to contribute to this character.



Given the fact that most biomacromolecules function in aqueous environments, developing water-soluble chirality sensors based on synthetic oligomers/polymers has also been targeted. Water-soluble synthetic oligoresorcinols (**26–28**)<sup>29</sup> were reported to self-assemble into single helical conformations in alkaline aqueous solutions and were applied as chirality sensor for chiral guests (Fig. 7). **28** adopted double helices at low pH, which dissociated into single strands with increasing pH due to deprotonation of the phenolic protons as confirmed by <sup>1</sup>H NMR. However, 8, 5 and 2 OH-protons remained bound to **28**, **27** and **26** even in the presence of excess NaOH because of their high *pK<sub>a</sub>* of >12. The oligoresorcinols adopted all *cisoid*-conformations through intramolecular hydrogen bonds between the phenoxide anions and the neighboring hydroxyl groups of the contiguous 2,2'-biphenol units. Addition of optically active ammonium (*S*)-**29** induced a bias in the helical sense of **28**, verified by the red-shift of the absorption at 331 nm as well as by the ROESY spectra. Binding of (*R*)-**29** and (*S*)-**29** induced mirror-imaged CD signals between 250–400 nm, which increases upon cooling from 25 to 0 °C. Short oligomer **26** generated almost no CD signal, implying that a minimum number of units in the oligomer is needed for the effective binding and the helical bias induction by the chiral guest molecules.

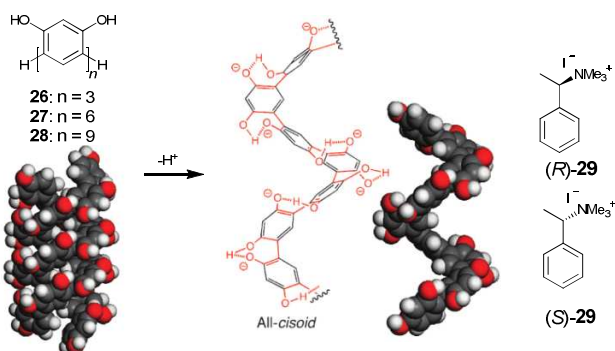
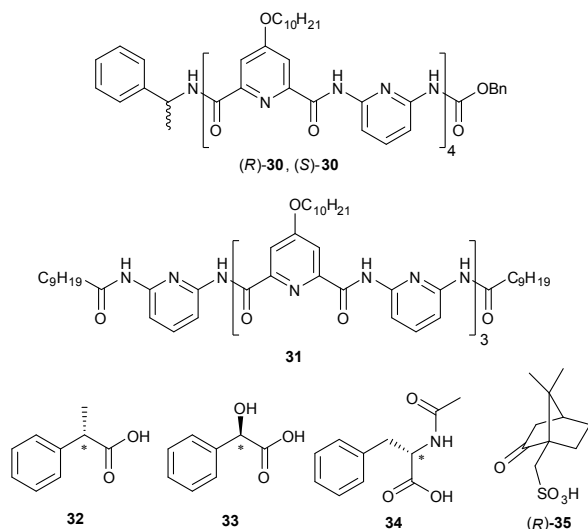


**Fig. 7** Chemical structure of oligoresorcinol polymers **26**, **27**, **28**, guest molecules (*R*)-**29** and (*S*)-**29** and the schematic diagram of the interconversion between double helix and single helix. (Reprinted with permission from *Chem. Commun.*, 2009, 1650–1652. Copyright 2009 RSC).

In terms of the chiral induction it can be either intermolecular or intramolecular or both. This was shown from the work of Huc *et al.*<sup>30</sup> Octamer **30** containing chiral (*R*)-or

(*S*)-phenylethylamine group and achiral heptamer **31** were designed to verify the intramolecular and intermolecular chiral induction, respectively. Intramolecular chiral induction was confirmed to occur in octamer (*R*)-**30** and (*S*)-**30** by their CD spectra that featured two mirror-imaged CD signals at 270 nm and 322 nm, respectively, relating to the electronic transitions of pyridine chromophore. The preference of *M*- or *P*-helix led by the chirality induction was further characterized by <sup>1</sup>H NMR. The ratio of the right- and left-handed helical diastereomers of octamer (*R*)-**30** was *ca.* 70:30 with a diastereometric excess of 40% at 10 °C. When achiral heptamer **31** was titrated by (*S*)-phenylpropionic acid **32**, <sup>1</sup>H NMR signals of two amide protons shifted to downfield by 0.4 ppm and 0.15 ppm, respectively, which was attributed to two hydrogen bonds between peripheral acylaminopyridine units of heptamer **31** and carboxylic acid. Two positive CD bands were observed at 270 and 322 nm when (*S*)-phenylpropionic acid was titrated towards heptamer **31**. Excessive acid however slowly decreased the CD intensity, suggesting partial unfolding of heptamer **31**. The fact that the same CD bands were observed in the cases of intra- and inter-molecular chirality induction indicates the identical handedness induced in the synthetic oligomers. (*R*)-Mandelic acid **33** led to similar induced CD bands in **31**, implying that the same chirality induction mechanism operates. Titrations by (*R*)-camphorsulfonic acid **35** generated a more intense ICD signal at 1 eq., while the signal at 322 nm vanished and a new CD band was observed quantitatively at 290 nm. This was explained in terms of strong protonation of the diacylaminopyridines by (*R*)-camphorsulfonic acid that causes conformation rearrangement in the oligomer. As chiral octamer (*S*)-**30** also contains “free” diacylaminopyridines for binding external chiral acids, besides the chiral phenylethylamine group, intermolecular handedness may also be induced. Titration by chiral acids **32–34** towards octamer (*S*)-**30** showed no significant further effect on the CD signal from the “free” diacylaminopyridines region, showing that the intramolecular induction is more efficient than the intermolecular one. This may relate to the fact of less chance of observing chiral amplification in cases of achiral foldamers upon binding to chiral analytes, probably because the bias energy barrier between the *P*- and *M*-helices of the foldamers is not too high. With limited examples available, it is still too early to conclude if with these foldamer based sensors there would be a minimum number of repeating unit and an optimal rigidity of the backbone that would be needed to ensure good performance.



Another interesting chirality sensing ensemble utilizing oligomeric structures (Fig. 8) was developed by Tanaka and Matile,<sup>31</sup> where the oligomeric structure was not responsible for chiral recognition but forming the transmembrane pores. The sensing ensemble consists of egg yolk phosphatidylcholine (EYPC) vesicles entrapping self-quenched carboxyfluorescein (CF) dye, pore-forming molecule **36** and enzyme Subtilisin Carlsberg, for *ee* assays of polyglutamate. Rigid rod-like oligophenyl compound **36** with  $\beta$ -strand side chains is driven by intermolecular hydrogen bonding between the  $\beta$ -strands rolls into an oligomeric barrel-shaped pore in the lipid bilayer. The inner barrel surface contains cationic histidine and lysine residues that create pore blockage by poly-anionic guests such as polyglutamates. Stereospecific enzymatic reaction breaks down poly-L-glutamate, but not poly-D-glutamate, into monomeric glutamate now as a poor pore blocker, pore blockage therefore occurs only significantly for poly-D-glutamate. Without pore blockage, the self-quenched CF dye would be released from inside the vesicles through the pore, resulting in recovery of its fluorescence due to dye dilution. The rate of CF fluorescence enhancement of vesicle solutions treated with **36** following an enzymatic reaction thus reports *ee* of the polyglutamate analyte. Similar to the above-mentioned CB[7] assay that also relies on enzymatic reactions (Fig. 2), *ee* value up to 99.9% can be accurately determined, again partly owing to the stereospecificity of the enzymatic reaction. Although this assay is limited for polyglutamate *ee* sensing, it provides an attractive approach of combining enzymatic reaction with synthetic membrane transport system constructed by synthetic oligomer, for sensing high *ee* close to 100%. This may be regarded as a dynamic macrocycle sensor.

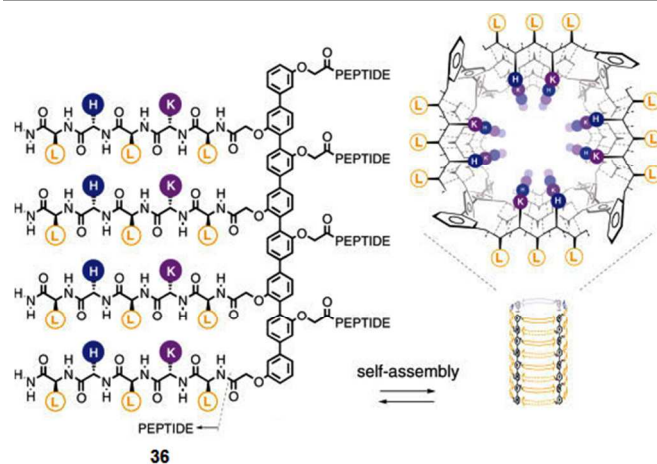


**Fig. 8** Transmembrane pore formed by self-assembly of **36** in lipid bilayer that allows efflux of self-quenched carboxyfluorescein (CF) dye loaded in the vesicles. (Reprinted with permission from *Chirality*, 2008, **20**, 307-312. Copyright 2008 Wiley-VCH).

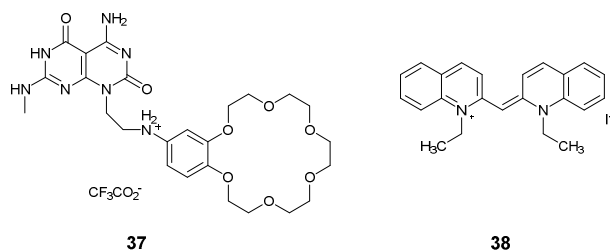
It shall be pointed out that, although none of the foldamers discussed in this *Review* has yet been applied for chirality sensing, possibly due to the limited scope of chiral guest molecules that can interact with the foldamers, the structural framework and the design methodology demonstrated in those systems should provide useful guidance for developing foldamer-based chirality sensors, if a suitable analyte binding site, for example, an aldehyde group, and/or a chromophore could be attached.

### Supramolecular polymers

Differing from synthetic oligomers/polymers, the building blocks of supramolecular polymers are held together by noncovalent interactions such as hydrogen bond, aromatic  $\pi$ -stacking, and metal coordination.<sup>32</sup> The ease of rationally designed building blocks to self-assemble into highly ordered helical superstructures in the presence of a chiral species in principle allows simple sensor design that the chiral analyte induces the sensor molecule to undergo a helical aggregation. The monomer-polymer equilibrium due to reversibility of the noncovalent interactions endows supramolecular polymers with stimuli-responsive properties,<sup>33</sup> which has been exploited for designing chemical sensors based on analyte-modulated aggregation.<sup>34</sup>

Fenniri group reported in 2002 an elegant example of chiral guest induced supramolecular chirality – helical rosette nanotubes formed by **37** with amino acid inducible chirality, although the system has not been exploited for *ee* sensing.<sup>35</sup> The bicyclic base (GC base, fused by guanine and cytosine) motif in **37** forms a six-membered supermacrocycle in water stabilized by 18 hydrogen bonds, which further aggregates into a tubular architecture driven by the strong hydrophobic interaction. Attaching to GC base by 18-crown-6-ether moiety provides a binding site for amino acids and the possibility of the hierarchical self-assemblies to be influenced by the amino acid via host-guest interaction. An ICD signal was indeed

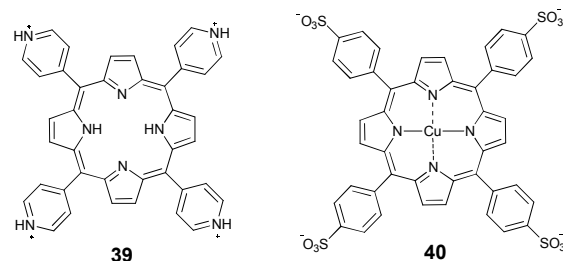
recorded upon the addition of *L*-/*D*-alanine. The hierarchical assemblies show induced chirality under the condition that the crown ethers fully bind to *L*-/*D*-alanine, which reveals the all or none nature of the supramolecular aggregates. When a mixture of *L*- and *D*-alanine is added to the rosette nanotubes, the supramolecular chirality is totally generated by the enantiomer of higher concentration, supporting the proposed autocatalytic mechanism of this process, whereas lower concentration enantiomer cannot express its chirality at the nanotubular level. The hydrophobic effect of the crown ether group allows small, aromatic, and hydrophobic amino acids to bind more easily to the GC base derivative **37** compared to the other larger and hydrophilic amino acids. This offers an efficient approach for chirality sensing of amino acids.



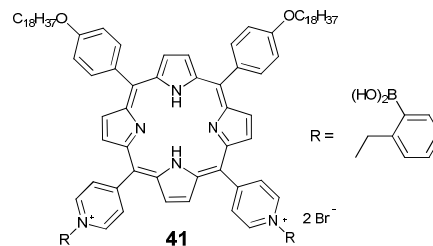
He *et al.*<sup>36</sup> established a chirality-sensing system based on pseudoisocyanine (PIC, **38**) aggregates. Achiral PIC **38** is known to form J-type aggregates, with its critical aggregation concentration in water tuneable by salt concentration. In the presence of *L*-/*D*-phenylalanine, ICD signal of PIC J-aggregates was observed in aqueous NaCl solution, the intensity of the Cotton effect being remarkably enhanced with increasing concentration of *L*-/*D*-phenylalanine. The ICD signal as a function of *ee* of phenylalanine exhibits the “majority-rules” effect, *i.e.* the chiral amplification. In addition, the chiral J-aggregates induced by *D*-tryptophan show opposite ICD signals to those led by *D*-phenylalanine, suggesting that the helicity of the chiral J-aggregates depends on the side group of aromatic amino acid.

Columnar porphyrin aggregates are also employed for chirality sensing. In the work of Watarai and co-workers,<sup>37</sup> tetracationic porphyrin, protonated form of 5,10,15,20-tetra(4-pyridyl)-21*H*,23*H*-porphine **39** is dissolved in an organic phase. Tetraanionic porphyrin, the deprotonated form of Cu(II)-*meso*-tetrakis-(4-sulfophenyl)prophine **40**, is facilely dispersed in an acidic aqueous phase of pH 2.3. Mixing of them occurs at toluene/water interface, leading to the formation of heteroaggregates consist of **39** and the same amount of **40**. When phenylalanine is introduced to the aqueous phase, centrifugal liquid membrane-circular dichroism (CLM-CD) spectra of the heteroaggregates reflect the absolute configuration of the amino acid. The sign of the CD signal of the heteroaggregates formed at liquid-liquid interface is determined by the chirality of phenylalanine, while it is almost not detected from the organic or aqueous phase, which means that chiral heteroaggregates are only formed at the interface. The linear correlation between the CD signal at 410 nm and *ee*

of phenylalanine, which means the absence of chiral amplification, allows the measurement of the chiral purity of a phenylalanine sample. Chirality of tyrosine and tryptophan can also be analyzed by the same interfacial chirality induction strategy, although the sensitivity is lower than that for phenylalanine.

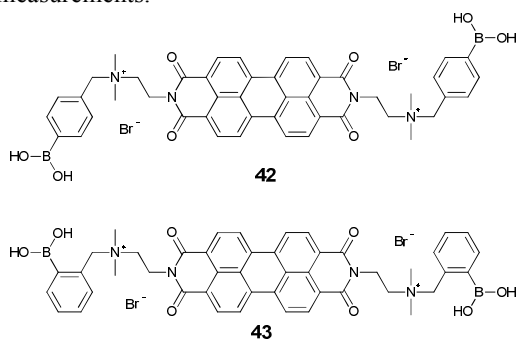


Combining porphyrin aggregation with reversible covalent bonding between boronic acid and *cis*-diol, new systems were developed for cooperative molecular recognition of saccharides. Shinkai *et al.*<sup>38</sup> developed a saccharide sensing scheme using porphyrin **41** aggregates. The boronic acid groups in **41** allow reversible interactions with saccharides. Helical porphyrin aggregates formed in aqueous solutions reflect the chirality of the added saccharide. By carefully comparing the absolute configuration of the tested monosaccharides and the sign of the exciton coupling CD signals, it was deduced that the helical orientation in the porphyrin-based aggregates is totally controlled by the direction of the 1,2-diol group in the furanose or pyranose form of the saccharide molecule. The system in principle should be applicable to *ee* sensing for saccharides, despite not examined.

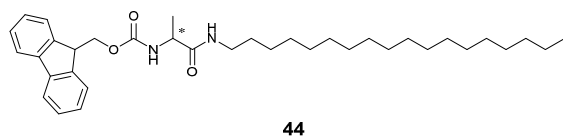


Employing aggregation of perylenebisimide (PBI) dyes in aqueous solutions and the interaction of boronic acids with diols, a new system for assays of *ee*, identity, and concentration of  $\alpha$ -hydroxy carboxylates was explored by Jiang *et al.*<sup>39</sup> Achiral PBI dyes **42** and **43** bearing *para*- and *ortho*-phenylboronic acid groups exist in small dimers or oligomers in the absence of analyte, yet forms large aggregates upon binding with  $\alpha$ -hydroxy carboxylate guests, leading to a decrease in perylene absorption around 500 nm. Meanwhile, the formed aggregates were optically active as shown by the strong bisignate ICD signal from the achiral perylene chromophore, which affords the capacity of *ee* determination by CD for seven  $\alpha$ -hydroxy carboxylates that bear no chromophore. The profile of the ICD spectrum is characteristic of the configuration of  $\alpha$ -hydroxy carboxylates, which was successfully used for analyte chirality differentiation following a linear discriminant analysis (LDA). With most of the tested  $\alpha$ -hydroxy carboxylates a linear CD-*ee* relationship was found. In two cases, however, nonlinear

dependence of CD intensity on analyte  $ee$  was observed, where a so-called opposite “majority-rules” was seen in that the slope is steeper at high  $ee$ . By combing the CD- $ee$  dependence and the analyte-induced absorption quenching, the concentrations and  $ee$ 's of “unknown” samples were calculated simultaneously with the average absolute error within  $\pm 2.1\%$ . Note that the boronic acid group that interacts with chiral analyte locates away from the chromophore by a long distance, yet an effective chirality induction was shown by the observation of coupled exciton CD signals. This example therefore highlights the potential of using induced helical aggregation of achiral dyes for CD measurement of  $ee$  of those chiral analytes that bear no chromophore or bear a chromophore but is far away from the chiral center. This expands the scope of application in chirality sensing of the classic CD spectroscopy that normally requires the presence of a chromophore next to the chiral center for direct measurements.

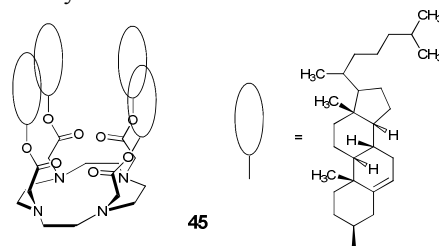


An interesting variation of the chirality induction approach in supramolecular polymers, is not by using achiral monomer but by a racemic mixture of enantiomers.<sup>40</sup> *N*-Fmoc-L- and D-alanines, L-/D-**44**, can gelate in a variety of organic solvents, while the fibrous or flat nanostructures observed in SEM show no apparent chiral structure. SEM images of the gels formed from the racemic mixtures with a slight enantiomeric excess show however obvious chiral twist. The highest CD signal was observed in the gel formed by L-/D-**44** mixture of  $ee$  2%, whereas the signal started to drop beyond  $ee$  2%. This is different from the normal “majority-rules” active systems, despite the fact that the slope of CD signal versus  $ee$  is still steepest at 0%  $ee$ . This distinctive character of the racemic assemblies offers a new strategy for chirality sensing. Upon introduction of a small amount of amino acid derivatives to the racemate, a strong CD signal was observed since the perturbation of the added species leads to diastereoselective aggregation. This affords an extremely sensitive supramolecular chirality sensing system for protected amino acids of  $ee$  close to 0.

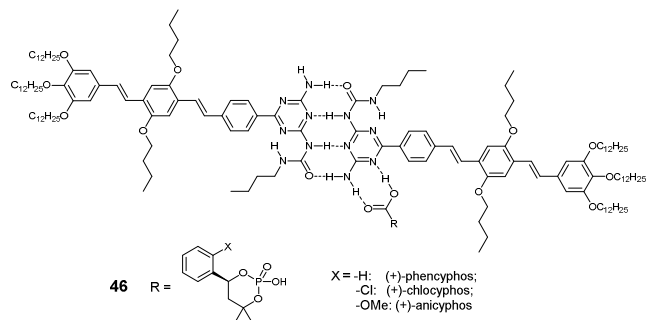


Macrocycle sensor has shown to selectively recognize a guest enantiomer as described in the previous section, its

aggregates also hold potential for chirality sensing at the supramolecular level. Tsukube group<sup>41</sup> designed a cholesterol-armed cyclen **45** for chiral recognition. The  $\text{Na}^+$ -**45** complex is amphiphilic and thus pertains to aggregate in aqueous solution with a critical aggregation concentration of  $4.0 \times 10^{-6} \text{ M}$  in 80/20  $\text{H}_2\text{O}/\text{EtOH}$  (pH 7.2), forming chiral hydrophobic cavity that allows chiral species to be extremely sensitively sensed even by using naked eyes to view the fluorescence of dansyl-L- and D-amino acid anions at  $10^{-7} \text{ M}$  level, with a L-/D-enantioselectivity of maximum 2.2. ICD signals of  $\text{Na}^+$ -**45** complex aggregates upon binding to dansyl-L- and D-amino acid anions exhibited opposite signs, correlating thereby the sign of the ICD signal to the absolute configuration of the amino acids. It is probably because of the too strong binding of both enantiomers, the enantioselectivity remains moderate.

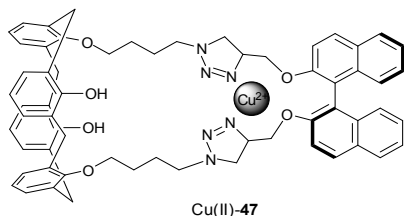


Oligo(*p*-phenylenevinylene)s (OPVs) which possess an extended  $\pi$ -conjugation are known for their optical and electronic properties. Molecular recognition driven self-assembly has been applied to organize dimers of **46** into helical OPV stack aggregates.<sup>42</sup> Saturation of CD signal was observed at a (-)-phenicyphos concentration well below stoichiometry, indicating the operation of a nonlinear effect, known as the “sergeant and soldiers principle”.<sup>43</sup> Moderate “majority-rules” effects were found, again showing chiral amplification. The resolution and detection of  $ee$  values apply well to other phenicyphos derivatives (chlocyphos and anicyphos) and mandelic acid.

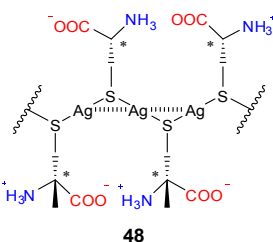


Apart from absorption, fluorescence, NMR and CD, dynamic light scattering technique (DLS) can be used for chirality sensing when employing supramolecular polymers. Li and coworkers<sup>44</sup> reported that chiral R-1,1-bi-2-naphthol-derived calix[4]arene **47** undergoes analyte-dependent aggregation. Calixarene framework in the aggregates and appending chiral binaphthyl groups provide a chiral space for binding of chiral analyte. Fluorescence of **47** is quenched effectively by Cu(II) and it recovers when mandelic acid (MA)

is introduced, depending on the identity of the MA enantiomers. The limit of the detection for chiral discrimination of MA is  $2 \times 10^{-5}$  M by using fluorescence assay. The absolute configuration of MA is also reflected in the nanostructure of the self-assembly of Cu(II)-**47** complex. Mixture of Cu(II)-**47** complex and (*R*)-MA are organized to larger aggregates than that of Cu(II)-**47**/(*S*)-MA. The difference in size distribution of the enantiomeric aggregates allows sensitive detection by DLS. The detection limit ( $2 \times 10^{-7}$  M) is improved by 100-fold compared to that of the fluorescence assay.



Coordination polymers were also exploited for chirality sensing. By mixing Ag(I) and cysteine (Cys) in aqueous solutions, coordinate polymers **48**<sup>45</sup> with repeating unit of Ag(I)-Cys form. The self-assembly occurs immediately in aqueous solution at pH 5, thanks to the argentophilic<sup>46</sup> and electrostatic interactions. Limit of detection for Cys is at micromolar level using absorption and CD signalling, while the molecular chirality of Cys is reflected by the sign of the induced CD signal, which also enables *ee* measurements when L- and D-Cys mixtures of varying *ee* are employed. Other amino acids cannot produce noticeable signals related to Ag(I)-Ag(I) interaction at *ca.* 350 nm. A highly sensitive and selective, yet simple method for chirality sensing for Cys was thus established. Note that the CD and absorption signals related to the Ag(I)...Ag(I) interactions appear in the wavelength window where the ligand and Ag(I) give no signal, thus assuming a zero-background sensing system. Similar metallophilic interaction also occurs with other  $d^{10}/d^8$  transition metal ions such as Au(I), Cu(I), Pt(II) and Pd(II),<sup>46</sup> chirality sensing using this concept shall be applicable to a broad scope of chiral analytes when the chiral analyte is equipped with a thiol (-SH) or pyridine group. Using luminescent rare-earth metal ion directed chiral assembly in solutions or in Langmuir-Blodgett films were also shown.<sup>47</sup> This forms another basis of chirality sensing using metal complexes that would find applications in chirality sensing.



Chirality sensing in supramolecular systems are not limited to the solution phase, supramolecular gel is also a potential

medium for discrimination of chiral species. A supramolecular chirality sensing system for phenylalanine (Phe) has been designed by Zhang *et al.*<sup>48</sup> By simply mixing two equivalents of Phe and one equivalent of Cu(II), supramolecular hydrogel of the Cu(II)-Phe complex is formed (Fig. 9). Judging from the CD signals of the d-d transition of Cu(II), absolute configuration of Phe can be identified in the CD spectra of the corresponding xerogels. The gelation ability of the 2Phe-Cu metallogelator critically depends on *ee* of Phe. Full hydrogel state can be obtained when *ee* value is higher than 80%, while the hydrogel collapses if the *ee* value is lower than 30%. This supramolecular system is stabilized by intermolecular hydrogen bonding, coordination of carboxylic/amino groups toward Cu(II), hydrophobic and/or  $\pi$ - $\pi$  stacking interactions. In according with this assumption, no gelation was observed by replacing aromatic Phe with other amino acids. This establishes a new platform using supramolecular hydrogel for chiral sensing and recognition.

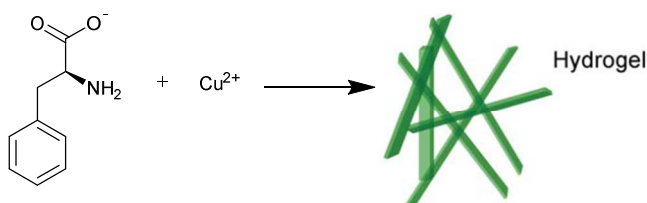


**Fig.9** Schematic illustration of supramolecular metallogel formation via Phe coordinating with Cu(II). (Reprinted with permission from *Dalton Trans.*, 2010, **39**, 7054-7058. Copyright 2010 RSC).

## Nanoparticles

Nanoparticles in general act as both signal reporter and the framework to immobilize chiral ligands. Size and shape of the nanoparticles therefore represent important parameters for their performance since they not only define the optical properties, but also the density and relative orientations of the ligands on the particle surface that are critical for their interactions with chiral analytes.

Uridine 5'-triphosphate (UTP) capped silver nanoparticles (Ag NPs, Fig. 10) have been prepared for chirality sensing of Cys.<sup>49</sup> Difference in the interactions of D- and L-Cys with modified Ag NPs is displayed in the UV-Vis absorption. Upon introduction of D-Cys, the yellow solution of Ag NPs rapidly turns red with a remarkable change in the absorption spectra, because of the D-Cys induced aggregation of Ag NPs. The same phenomenon does not occur when L-Cys is applied, implying that L-Cys is unable to induce the aggregation. The striking difference in the absorption spectra of the Ag NPs solution containing D- and L-Cys therefore enables enantiodiscrimination of Cys. Furthermore, enantioselective separation and enantiomeric purification were made possible by centrifuging the solution of Ag NPs with racemic Cys. The precipitates consist of UTP-capped Ag NPs and D-Cys that can be collected while L-Cys remains in the solution. With no need

of CD measurement, chirality sensing can be easily monitored even by naked eyes.

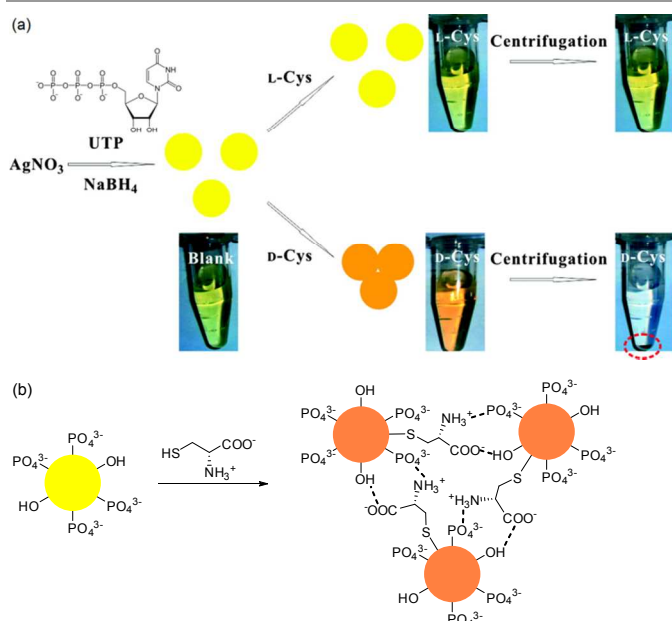


**Fig.10** (a) Colorimetric discrimination of L- and D-Cys using UTP-capped Ag NPs. (Adapted with permission from *Anal. Chem.*, 2011, **83**, 1504-1509. Copyright 2011 ACS). (b) A possible mechanism for D-Cys induced aggregation of UTP-capped Ag NPs.

Another colorimetric sensor for chiral discrimination of histidine (His) using Ag NPs was reported from Li group.<sup>50</sup> The Ag NPs clusters, L-Arg-ZnTPPS-Ag NPs (Fig. 11), were obtained by simply mixing the sulfonated zinc tetraphenylporphyrin (ZnTPPS) modified Ag NPs and L-arginine (L-Arg). L-Arg not only provides a chiral recognition site, but assembles ZnTPPS-Ag NPs into clusters, via its coordination to ZnTPPS. The Ag NPs clusters exhibit stronger recognition ability to His and methionine (Met) than to other amino acids. However, only L-His can induce assembly of L-Arg-ZnTPPS-Ag NPs. An obvious colour change occurs during L-His induced aggregation, while D-His hardly leads to any colour change. The induced aggregation was assumed to result from the interaction of the carboxylate, amine and imidazole groups of His with the L-Arg-ZnTPPS-Ag NPs. The induced CD signal at 200 nm can be used for empirical assignment of the absolute configuration of His.

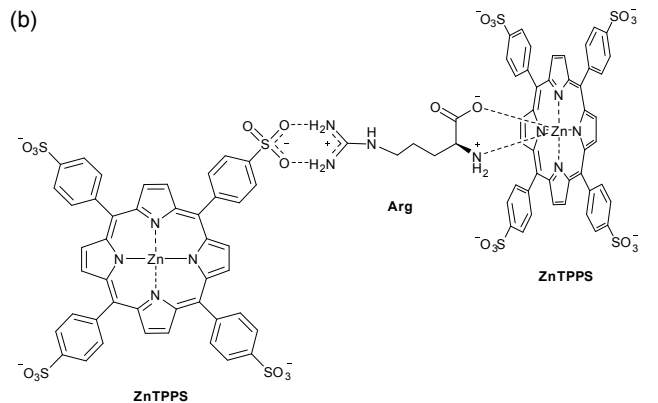
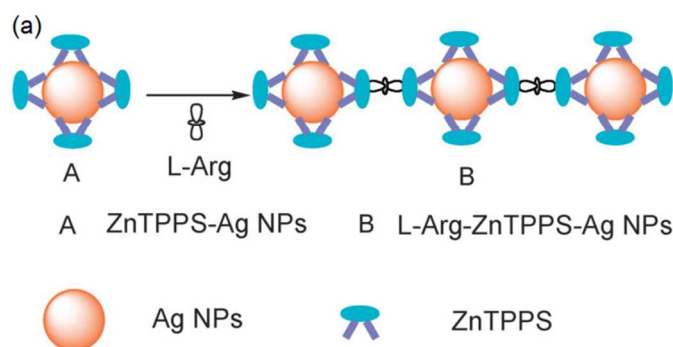


**Fig.11** (a) Route to L-Arg-ZnTPPS-Ag NPs cluster. (Reprinted with permission from *New J. Chem.*, 2012, **36**, 1442-1444. Copyright 2012 RSC). (b) Interaction of Arg with ZnTPPS of ZnTPPS-AgNPs leading to crosslinking of the NPs.

A fluorescent nanoparticle-based sensor was similarly developed for resolution of L/D-enantiomers. Aggregation of L-/D-Cys decorated CdTe quantum dots (L-/D-QDs) and gold nanorods (GNRs) were investigated by Xia *et al.*<sup>51</sup> When D-Cys is introduced into the mixture of L-QDs and GNRs, a dynamic nanoparticle-nanorod assembly is formed, leading to quenching of the fluorescence of the QDs by 74%. In contrast, adding L-Cys to the mixture of L-QDs and GNRs only results in a slight or negligible change in the fluorescence. This implies that heterochiral interaction results in more notable fluorescence quenching than the homochiral interaction, which is further confirmed by the likewise assembly L-/D-Cys in the presence of the D-QDs and GNRs. Not only can L-/D-Cys be directly quantified by fluorescence responses, the *ee* of the racemic Cys can be detected by the intensity of fluorescence as well.

Plasmonic chirality from the plasmonic nanoparticle dimers was also chosen as a candidate for chirality sensing.<sup>52</sup> Through covalent binding between Au and S atoms, Au NP dimers are assembled in the presence of Cys (Fig. 12). The Au NP dimers prepared by L-Cys and D-Cys, respectively, exhibit distinguished induced plasmon-chirality as shown by their CD signals, allowing therefore a selective chirality sensing of Cys, since only a slight change in the CD signal is observed when other amino acids are introduced. It appears that the nanoparticles based chirality sensing is more straightforward as naked eyes may see the difference in the changes of color or luminescence when individual enantiomer is introduced. Despite the possible difficulty in obtaining reproducible nanoparticles as in the case of polymers, developments of nanoparticles based chirality sensors are promising, considering the fact that robust methodologies are available for the synthesis and fabrication of nanoparticles of varying size and shape.

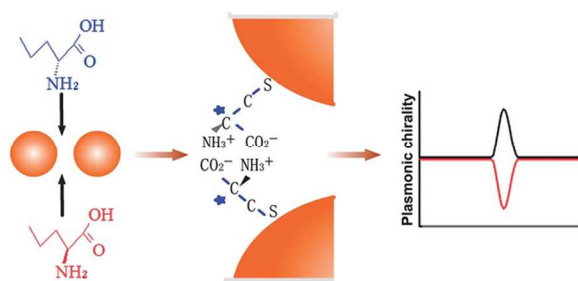


**Fig. 12** Schematic representation of chiral recognition of Cys enantiomers based on multiplex attractive forces. (Adapted with permission from *J. Mater. Chem. B*, 2013, **1**, 4478–4483. Copyright 2013 RSC).

## Conclusions and Remarks

We summarized four classes of chirality sensing systems that operate considerably differently from the traditional way of using small molecule-based sensors in terms of design strategy and/or sensing mechanism. These four chirality sensing systems are employing macrocycles, synthetic oligomers/polymers, supramolecular polymers and nanoparticles based sensors. It should be emphasized that the developments of these supramolecular chirality sensing systems benefit very much from the accumulation of knowledge of small-molecule based chirality sensing. A major advantage of the supramolecular chirality sensor is the possibility of signal amplification because multivalent interactions may occur between these sensors and the chiral analytes. The diversity of structural frameworks that can be employed and facilely made offers more chances for creating such sensors.

In order to render these supramolecular optical chirality sensing systems readily applicable for real analysis, for example for high throughput screening (HTS), three challenges need to be addressed. First, the scope of chiral analytes is typically limited to certain classes of compounds with reactive groups to form metal complexes or dynamic covalent bonds, such as amines, aldehydes, carboxylic acids, and alcohols, while a large portion of the synthetic reaction products do not contain those functional groups. In this regard, Nau's cucurbituril-dye ensemble strategy (Fig. 3) stands out as it only requires an aromatic moiety for the analyte to interact within the macrocyclic cavity, and thus expands the scope of the chiral analyte. Given the availability of many other macrocyclic sensory frameworks such as calixarene, calixpyrrole, calixresorcinarenes<sup>10,11</sup> and even the recently actively investigated cycloparaphenylenes,<sup>53,54</sup> this strategy could have more extension in designing chirality sensors for a broader scope of analytes. Similarly more chirality sensing systems can be designed utilizing noncovalent interactions, in particular the recently actively investigated halogen bonding.<sup>55</sup> In these cases the dynamic characters of the noncovalent interactions may raise an issue of reproducibility of the formed supramolecular ensembles such as supramolecular polymers and ligand protected/stabilized nanoparticles, that deserves further efforts.

Second, precisely measuring *ee* close to 100% is of greater interest in asymmetric syntheses, yet this has been scarcely realized using optical sensors. Two examples with a capacity of sensing high *ee*<sup>8,14</sup> are described in this Review, albeit based on stereospecific enzymatic reactions that would have a severely limited analyte scope and require careful optimization of the reaction conditions. A strategically straightforward but challenging-to-achieve approach is to enhance the absolute CD intensity in the chirality induction approach using an achiral sensor or the enantioselectivity of a chiral sensor. Alternatively, the strategy of exploiting “majority-rules” active polymers by adding an equal equivalent of opposite enantiomer seems promising,<sup>18</sup> while the limitation of needing the knowledge of the analyte concentration could probably be removed by chemometric methods. Finally, synthetic difficulty should be taken into account to render the chirality sensor readily available for real applications. Easily synthesizable sensors can be designed, taking the supramolecular polymer approach as an example, by simply attaching an analyte binding site to a chromophore capable of aggregation, without the need for more prudent consideration in the position of the analyte binding site which is often the case with small molecule based sensors.

It shall be noted that the investigation into these four classes of chirality sensors remains quite young, detailed systematic explorations are needed to optimize structural and medium parameters that define the chirality sensing performance. For example, for oligomer/polymer based sensors, whether there are minimum sizes of them and optimal rigidity of the backbone that, together with the choice of suitable solvent(s), could ensure a good performance. We believe that with the huge basis of knowledge we have at hands of the small molecular based chirality sensors, chirality sensing strategies discussed here would grow mature and help to produce highly sensitive and facile chirality sensors eligible for real applications.

## Acknowledgements

This is a part of the themed issue of “Sensor Targets and Imaging Agents”. We thank the support of the MOST (2011CB910403), NSFC (91127019, 21275121, 21435003), and the Program for Changjiang Scholars and Innovative Research Team in University, the MOE of China (IRT13036).

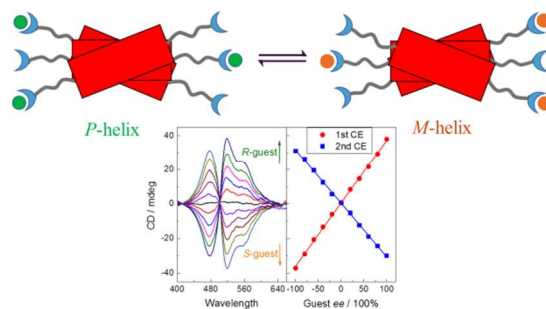
## Notes and references

- X. Zhang, J. Yin and J. Yoon, *Chem. Rev.*, 2014, **114**, 4918–4959.
- H. H. Jo, C.-Y. Lin and E. V. Anslyn, *Acc. Chem. Res.*, 2014, **47**, 2212–2221.
- C. Wolf and K. W. Bentley, *Chem. Soc. Rev.*, 2013, **42**, 5408–5424.
- J. Labuta, S. Ishihara, T. Šikorský, Z. Futera, A. Shundo, L. Hanyková, J. V. Burda, K. Ariga and J. P. Hill, *Nat. Commun.*, 2013, **4**.
- J. Labuta, S. Ishihara, A. Shundo, S. Arai, S. Takeoka, K. Ariga and J. P. Hill, *Chem. Eur. J.*, 2011, **17**, 3558–3561.
- A. Shundo, J. Labuta, J. P. Hill, S. Ishihara and K. Ariga, *J. Am. Chem. Soc.*, 2009, **131**, 9494–9495.

7. M. V. Rekharsky, H. Yamamura, C. Inoue, M. Kawai, I. Osaka, R. Arakawa, K. Shiba, A. Sato, Y. H. Ko, N. Selvapalam, K. Kim and Y. Inoue, *J. Am. Chem. Soc.*, 2006, **128**, 14871-14880.
8. D. M. Bailey, A. Hennig, V. D. Uzunova and W. M. Nau, *Chem. Eur. J.*, 2008, **14**, 6069-6077.
9. F. Biedermann and W. M. Nau, *Angew. Chem. Int. Ed.*, 2014, **53**, 5694-5699.
10. P. Shahgaldian and U. Pieleas, *Sensors (Basel, Switzerland)*, 2006, **6**, 593-615.
11. J. L. Sessler, P. A. Gale and W.-S. Cho, in *Anion Receptor Chemistry*, RSC publishing, Cambridge, UK, 2006, pp. 131-170.
12. K. Nonaka, M. Yamaguchi, M. Yasui, S. Fujiwara, T. Hashimoto and T. Hayashita, *Chem. Commun.*, 2014, **50**, 10059-10061.
13. X. Wu, L.-R. Lin, Y.-J. Huang, Z. Li and Y.-B. Jiang, *Chem. Commun.*, 2012, **48**, 4362-4364.
14. C. García-Ruiz, X. Hu, F. Ariese and C. Gooijer, *Talanta*, 2005, **66**, 634-640.
15. M. M. Green, B. A. Garetz, B. Munoz, H. Chang, S. Hoke and R. G. Cooks, *J. Am. Chem. Soc.*, 1995, **117**, 4181-4182.
16. R. Nonokawa and E. Yashima, *J. Am. Chem. Soc.*, 2002, **125**, 1278-1283.
17. M. Morimoto, K. Tamura, K. Nagai and E. Yashima, *J. Polym. Sci., Part A: Polym. Chem.*, 2010, **48**, 1383-1390.
18. H. M. Seifert, Y.-B. Jiang and E. V. Anslyn, *Chem. Commun.*, 2014.
19. T. Shiraki, A. Dawn, Y. Tsuchiya, T. Yamamoto and S. Shinkai, *Chem. Commun.*, 2012, **48**, 7091-7093.
20. G. Fukuhara and Y. Inoue, *Chem. Eur. J.*, 2012, **18**, 11459-11464.
21. K. Maeda, H. Mochizuki, K. Osato and E. Yashima, *Macromolecules*, 2011, **44**, 3217-3226.
22. D.-W. Zhang, X. Zhao and Z.-T. Li, *Acc. Chem. Res.*, 2014, **47**, 1961-1970.
23. J.-L. Hou, X.-B. Shao, G.-J. Chen, Y.-X. Zhou, X.-K. Jiang and Z.-T. Li, *J. Am. Chem. Soc.*, 2004, **126**, 12386-12394.
24. C. Li, G.-T. Wang, H.-P. Yi, X.-K. Jiang, Z.-T. Li and R.-X. Wang, *Org. Lett.*, 2007, **9**, 1797-1800.
25. M. Inouye, M. Waki and H. Abe, *J. Am. Chem. Soc.*, 2004, **126**, 2022-2027.
26. H. Abe, H. Machiguchi, S. Matsumoto and M. Inouye, *J. Org. Chem.*, 2008, **73**, 4650-4661.
27. J.-m. Suk, D. A. Kim and K.-S. Jeong, *Org. Lett.*, 2012, **14**, 5018-5021.
28. Y. Ferrand, A. M. Kendhale, B. Kauffmann, A. Grélar, C. Marie, V. Blot, M. Pipelier, D. Dubreuil and I. Huc, *J. Am. Chem. Soc.*, 2010, **132**, 7858-7859.
29. H. Goto, Y. Furusho and E. Yashima, *Chem. Commun.*, 2009, 1650-1652.
30. V. Maurizot, C. Dolain and I. Huc, *Eur. J. Org. Chem.*, 2005, **2005**, 1293-1301.
31. H. Tanaka and S. Matile, *Chirality*, 2008, **20**, 307-312.
32. T. F. A. De Greef, M. M. J. Smulders, M. Wolfs, A. P. H. J. Schenning, R. P. Sijbesma and E. W. Meijer, *Chem. Rev.*, 2009, **109**, 5687-5754.
33. T. Aida, E. W. Meijer and S. I. Stupp, *Science*, 2012, **335**, 813-817.
34. Y.-J. Huang, W.-J. Ouyang, X. Wu, Z. Li, J. S. Fossey, T. D. James and Y.-B. Jiang, *J. Am. Chem. Soc.*, 2013, **135**, 1700-1703.
35. H. Fenniri, B.-L. Deng and A. E. Ribbe, *J. Am. Chem. Soc.*, 2002, **124**, 11064-11072.
36. L. Zeng, Y. He, Z. Dai, J. Wang, C. Wang and Y. Yang, *Sci. China, Ser. B*, 2009, **52**, 1227-1234.
37. H. Takechi and H. Watarai, *Chem. Lett.*, 2011, **40**, 303-305.
38. S. Arimori, M. Takeuchi and S. Shinkai, *J. Am. Chem. Soc.*, 1996, **118**, 245-246.
39. X. Wu, X.-X. Chen, B.-N. Song, Y.-J. Huang, Z. Li, Z. Chen, T. D. James and Y.-B. Jiang, *Chem. Eur. J.*, 2014, **20**, 11793-11799.
40. H. Cao, X. Zhu and M. Liu, *Angew. Chem. Int. Ed.*, 2013, **52**, 4122-4126.
41. S. Shinoda, T. Okazaki, T. N. Player, H. Misaki, K. Hori and H. Tsukube, *J. Org. Chem.*, 2005, **70**, 1835-1843.
42. F. Riobe, A. P. H. J. Schenning and D. B. Amabilino, *Org. Biomol. Chem.*, 2012, **10**, 9152-9157.
43. M. M. Green, M. P. Reidy, R. D. Johnson, G. Darling, D. J. O'Leary and G. Willson, *J. Am. Chem. Soc.*, 1989, **111**, 6452-6454.
44. F. Miao, J. Zhou, D. Tian and H. Li, *Org. Lett.*, 2012, **14**, 3572-3575.
45. J.-S. Shen, D.-H. Li, M.-B. Zhang, J. Zhou, H. Zhang and Y.-B. Jiang, *Langmuir*, 2010, **27**, 481-486.
46. H. Schmidbaur and A. Schier, *Angew. Chem. Int. Ed.*, 2015, in press (doi: 10.1002/anie.201405936).
47. S. J. Bradberry, A. J. Savyasachi, M. Martinez-Calvo and T. Gunnlaugsson, *Coord. Chem. Rev.*, 2014, **273-274**, 226-241.
48. J.-S. Shen, G.-J. Mao, Y.-H. Zhou, Y.-B. Jiang and H.-W. Zhang, *Dalton Trans.*, 2010, **39**, 7054-7058.
49. M. Zhang and B.-C. Ye, *Anal. Chem.*, 2011, **83**, 1504-1509.
50. Y. Sun, L. Zhang and H. Li, *New J. Chem.*, 2012, **36**, 1442-1444.
51. L. Song, S. Wang, N. A. Kotov and Y. Xia, *Anal. Chem.*, 2012, **84**, 7330-7335.
52. L. Xu, Z. Xu, W. Ma, L. Liu, L. Wang, H. Kuang and C. Xu, *J. Mater. Chem. B*, 2013, **1**, 4478-4483.
53. E. Kayahara, V. K. Patel and S. Yamago, *J. Am. Chem. Soc.*, 2014, **136**, 2284-2287.
54. P. J. Evans, E. R. Darzi and R. Jasti, *Nat. Chem.*, 2014, **6**, 404-408.
55. M. J. Langton, S. W. Robinson, I. Marques, V. Félix and P. D. Beer, *Nat. Chem.*, 2014, **6**, 1039-1043.

TOC Entry

# Optical chirality sensing using macrocycles, synthetic and supramolecular oligomers/polymers, and nanoparticles based sensors

Zhan Chen,<sup>a</sup> Qian Wang,<sup>a</sup> Xin Wu,<sup>a</sup> Zhao Li<sup>a</sup> and Yun-Bao Jiang<sup>a,\*</sup>

Recent advance in four classes of non-small-molecule based chirality sensors is reviewed.

## Biography



---

Zhan Chen received his BS degree in chemistry from Xiamen University in 2008. From 2008 to 2014, he continued his scientific education as a PhD student under the guidance of Professor Yun-Bao Jiang in the same University. Part of his graduate research was performed at the Institute of Pharmacology & Toxicology, where he spent four months in the group of Professor Jian-Wei Xie in 2010. His research mainly focuses on chiral aggregation of perylenebisimide dyes.



Qian Wang received her BS degree in chemistry from Xiamen University in 2009. She has been a PhD graduate under the supervision of Professor Yun-Bao Jiang since then. She spent two years as a joint PhD student at Bowling Green State University in the United States under Professor H. Peter Lu. Her research focuses on spectroscopic investigations of self-assembly and interactions of bioactive macromolecules.



---

Xin Wu graduated from Xiamen University with a BS degree in Chemistry in 2011. He is currently a PhD graduate student under the supervision of Prof. Philip A. Gale (University of Southampton) and Prof. Yun-Bao Jiang (Xiamen University). His research focuses on sensing, self-assembly and lipid bilayer transport of biologically important species.



---

Zhao Li is an associate professor at Xiamen University. She completed her first degree in Chemical Engineering in 1989 at Jiangnan University. After obtaining her MS degree from Xiamen University in 1997 she joined the University as an assistant professor. She was awarded a PhD in 2008 for her work with Professor Yun-Bao Jiang and spent one year as a postdoctoral fellow with Dr. Hua-Qiang Zeng at the National University of Singapore before taking up her current position in 2009. Her current research interests are supramolecular chirality and sensing.



*Dr. Yun-Bao Jiang is a Chair Professor in the College of Chemistry and Chemical Engineering, Xiamen University, China. While his general research interests lie in the photophysics of electron/proton transfer and supramolecular chemical sensing and molecular recognition, chiral sensing is a subject of current interest. Dr. Jiang is an alumnus of Xiamen University, receiving his PhD in 1990. He was awarded the distinguished young investigator grant of NSFC in 2004 and has been Dean of the College since 2013.*